

FEATURES OF ELECTRONIC TRANSPORT IN RELAXED Si/Si_{1-x}Ge_x HETEROSTRUCTURES WITH HIGH DOPING LEVEL

L.K. Orlov^{1,2)}, A.A.Mel'nikova²⁾, M.L.Orlov^{1,2)}, N.A.Alyabina³⁾, N.L.Ivina²⁾, V.N.Neverov⁴⁾, and Zs.J.Horváth⁵⁾

¹⁾Institute for Physics of Microstructures, Russian Academy of Sciences, N.Novgorod, Russia,

²⁾Nizhny Novgorod State Technical University,

³⁾Nizhny Novgorod, Lobachevsky University,

⁴⁾Institute for Physics of Metals, Russian Academy of Sciences, Yekaterinburg, Russia,

⁵⁾Óbuda University, Institute of Microelectronics and Technology, Budapest, Hungary

Abstract

The low-temperature electrical and magnetotransport characteristics of partially relaxed Si/Si_{1-x}Ge_x heterostructures with two-dimensional electron channel ($n_e \geq 10^{12} \text{ cm}^{-2}$) in an elastically strained silicon layer of nanometer thickness have been studied. The detailed calculation of the potential and of the electrons distribution in layers of the structure was carried out to understand the observed phenomena. The dependence of the tunneling transparency of the barrier separating the 2D and 3D transport channels in the structure, was studied as a function of the doping level, the degree of blurring boundaries, layer thickness, degree of relaxation of elastic stresses in the layers of the structure. Tunnel characteristics of the barrier between the layers were manifested by the appearance of a tunneling component in the current-voltage characteristics of real structures. Instabilities, manifested during the magnetotransport measurements using both weak and strong magnetic fields are explained by the transitions of charge carriers from the two-dimensional into three-dimensional state, due to interlayer tunneling transitions of electrons.

Introduction

The electronic properties of Si/Si_{1-x}Ge_x transistor structures with two-dimensional transport channels in different layers of the heterostructure are discussed in the literature for quite a long time. However, the greatest success in the area of real transistor devices promoting in millimeter waves, is obtained mainly in strained planar heterostructures containing quantum layers of the Si_{1-x}Ge_x solid solution with electron or hole conductance [1-3]. Much less works are devoted to studying the properties of relaxed heterostructures with an electron transport channel in the silicon layers. Earlier the main efforts were concentrated on the analysis of the structural defect features in the grown heterocompositions [4,5] and on low-temperature magnetotransport measurements of two-dimensional electrons in the elastic - strained layers of Si [6,7]. Problems arising from the formation of conductive Si channels with high-mobility electron gas in the surface layer of the solid solution Si_{1-x}Ge_x, are connected to the necessity of introduction a plastic deformation area in the structure. This area should be controlled by the density of extended defects due to the heterojunction formed in the vicinity of three-dimensional network of misfit dislocations [8]. The formation takes place between the buffer layer of a solid solution and the silicon substrate. At the same time due to the uncontrolled multiplication of misfit dislocations, it is difficult to increase the percentage of germanium in the solid solution layers (above 30 at.%), if the depth of the quantum well formed in the layers of the Si/Si_{1-x}Ge_x heterostructure is increased.

Increasing the doping level in the Si/Si_{1-x}Ge_x transistor heterostructures leads to peculiar behavior of transport characteristics of these structures. These features are associated with the appearance of fundamental properties of the two-dimensional metal [6], and with quite a noticeable influence of the charge of free carriers' on the potential of the quantum well and adjacent barrier layers. The last fact was the main motivation for this work to discuss the regularities observed in experiments using partially relaxed Si_{1-x}Ge_x/Si/Si_{1-x}Ge_x transistor structures.

Experiment and calculations

The n⁺-SiGe/n-Si/p-SiGe double heterostructures with the two-dimensional silicon transport channel with a thickness of about 10 nm (Fig. 1) studied in the present work were characterized by the value of the surface carrier concentration $n_{cr} > 10^{12} \text{ cm}^{-2}$, and a relatively low values of electron mobility in the system ($\mu_e \approx 3000\text{-}5000 \text{ cm}^2/\text{Vs}$ at liquid helium temperature) [5]. The details of sample preparation is presented elsewhere [7]. The samples were studied by magnetoresistance, Hall and current-voltage measurements.

We have previously shown that the electrons in Si channel exert two-dimensional

properties at the presence of weak magnetic field even at relatively low mobility, partly related to participation of several groups of carriers from different layers in the transport. These properties are expressed, in particular, in the appearance of a negative magnetoresistance of the system described by the logarithmic type corrections to the conductivity and associated with the manifestation of weak localization [7].

The numerical analysis of potential and electron distribution in structure layers was carried out on the base of the Poisson equation and quasihydrodynamics equations for the better understanding of the observed patterns of our samples with the different character of the elastic strain in the layers and different levels of doping. The dependence of the shape of the potential barrier formed in the vicinity of the heterojunction and features formed in a layer of silicon quantum well on various parameters of the system, including the level of doping of the layers, their composition and the width of the quantum well was studied.

Calculation of the potential in the considered heterostructures orthogonally to the layer plane direction (below x axis) has been realized on the base of quasihydrodynamic and electrostatic equation system. Generally the complete differential equation system, which includes quasihydrodynamic continuity equations for the charges and currents and Poisson's equation, is submitted in the following form:

$$\begin{aligned} \operatorname{div}(j_e) &= R_e - G_e, & \operatorname{div}(j_h) &= R_h - G_h, \\ j_e &= e(\mu_e n_e E_x + D_e (dn_e/dx)), & j_h &= e(\mu_h n_h E_x - D_h (dn_h/dx)), & j &= j_n + j_p + j_s, \\ (d\phi^2/dx^2) &= (e/\epsilon\epsilon_0)(n_e + N_A - n_h - N_D). \end{aligned} \quad (1)$$

Here n_e and n_h are the electron and hole concentrations, respectively, in the given plane of the structure; G_e and G_h are the generation rate of the electrons and holes in a unit of volume due to the external factors; R_e and R_h are the recombination rates of the nonequilibrium charge carriers; j_e and j_h are the electron and hole current densities showing the magnitude of the leakage current in a transistor structure; ϕ is the electrostatic potential; N_A and N_D are the acceptor and donor concentrations, respectively, in the layers of an active part of the structure, which are determined by the problem specifications. In the frame of the used diffusion-drift model, μ_e and μ_h are the charge carrier mobility in the separate layers; E_x is an electric field density across the structure layers; D_e and D_h are the diffusion coefficients, relating to the μ_e and μ_h mobility by the Einstein relations. Offset current is assumed in the standard form:

$$j_s = eD_h n_{h0}/L_h + eD_e n_{e0}/L_e \quad (2)$$

where n_{h0} and n_{e0} are the equilibrium concentrations of the minority carriers, L_e and L_h are the electron and hole diffusion lengths, respectively. The basic equations are supplemented with the boundary conditions, chosen from the conditions of the electrical neutrality and thermodynamic

equilibrium on the contacts. Solution of the differential equation system (1) is obtained by a numerical method with the use of the Gummel scheme.

Structure of the potential and electron density distribution on system layers

The results of energy band structure calculations for the samples with the maximum strained ($\epsilon = 100\%$) and non-tensioned ($\epsilon = 0\%$) silicon layer in $n^+ - \text{Si}_{1-x}\text{Ge}_x / n - \text{Si} / p - \text{Si}_{1-x}\text{Ge}_x$ diode structure are presented in Fig. 2. In Fig. 2 area I corresponds to the top doped $n^+ - \text{Si}_{1-x}\text{Ge}_x$ layer, area II corresponds to the base n-Si layer, that forms an electron transport channel in the layer plane, area III corresponds to the buffer p- $\text{Si}_{1-x}\text{Ge}_x$ sublayer of the solid solution that separates the transport channel from the Si substrate. We used following parameter values in our model: $x = 0.25$, $N_D(\text{I}) = 2 \cdot 10^{18} \text{ cm}^{-3}$, $N_D(\text{II}) = 10^{13} \text{ cm}^{-3}$, $N_A(\text{III}) = 10^{13} \text{ cm}^{-3}$, $d(\text{I}) = 40 \text{ nm}$, $d(\text{II}) = 10 \text{ nm}$, $d(\text{III}) = 100 \text{ nm}$. The potential $\phi(x)$ calculation has been performed using a flat-band approximation for the top barrier solid solution layer. It is reasonable, because the Fermi level isn't pinned to the external contact, its position is determined by surface states.

The basic difference in the character of electron concentration distribution in the layers for the maximum value of an elastic relaxation ($\epsilon = 100\%$, $E_g(\text{Si}) = 0.93 \text{ eV}$, $E_g(\text{SiGe}) = 1.07 \text{ eV}$, $\Delta E_v = 0.056 \text{ eV}$) and for the absence of elastic relaxation ($\epsilon = 0\%$, $E_g(\text{Si}) = 1.1 \text{ eV}$, $E_g(\text{SiGe}) = 0.986 \text{ eV}$, $\Delta E_v = 0.178 \text{ eV}$) in the $\text{Si}_{0.75}\text{Ge}_{0.25}/\text{Si}$ layers of heterostructure are shown in Figs. 2.c and 2.d for doping level $N_D(\text{I}) = 2 \cdot 10^{18} \text{ cm}^{-3}$. The calculations were carried out for extreme cases of the plastic deformation indicated above using the published data [9]. The results show (Fig. 2) that two-dimensional potential well in the Si layer has a maximum depth at 100% relaxation of the elastic strain in the solid solution layers. The corresponding distribution of the electrons in the layers of the given sample is shown in Figs. 2 and 3.b. It is seen that electrons are localized in the neighborhood of only the upper border of the well and their concentration can substantially exceed the average level of doping of the top barrier layer. Si layer forms a two-dimensional transport channel in the structure. Electron concentration density in this layer exceeds the N_D concentration of the doping impurity in the top barrier SiGe layer. Reduction of the elastic stress in a Si layer as well as a decrease of the valence band offset on the interfaces at the absence of a plastic relaxation in the system, yield a decrease of the potential well depth and of charge carrier concentration in it for the same doping level.

It is important to estimate how the parameters of potential barrier $h_b = E_{ba} = E_b - E_a$ and quantum well $E_{dc} = E_d - E_c$, $\Delta E_c = E_{bc} = E_b - E_c$ (Fig. 3.a) will depend on the elastic relaxation of the Si layers and their doping level. We have calculated also the barrier width $W_b = x_f - x_e$ at its half maximum value relative to the bottom of conduction band in the top doped layer ($h_b/2$), and the width W_{qw} of quantum well on the heights h_b and $h_b/2$ relative to the bottom of conduction

band E_a near the top ohmic contact (Fig. 3.a). The characteristic shape of the energy band diagrams for the structures with different extent of elastic strain relaxation ϵ in the layers is shown on Fig. 3 and in a Table 1. The calculation shows a strong dependence of the potential characteristics formed in the vicinity of a silicon transport channel on a number of initial parameters of the system. Our calculations show that in the considered heterostructures with $x = 0.25$ even for an extreme case of maximum deformation of a Si layer, that correspond to the 100% relaxation of the elastic stress in the layers of the structure, quantum well depth for electron does not exceed the value $\Delta E_c \approx 190$ meV. Indeed, it is even smaller due to both the only partial relaxation of the elastic stress in the layers and to tunneling transparency of the potential barrier formed on the layers interface. One can note in Table 1 that the barrier width on its half-height ($h_b/2 = 73$ meV) is equal to $W_b \approx 1-2$ nm (Fig. 3).

Elastic relaxation in our samples is about 40-60%. So the real depth of the Si quantum well in the structure did not exceed 100 meV. The thinness of the formed barrier layer and the presence of the electric field in the potential well yield the deviation of its shape from the rectangular form. The ratio of the $dE_{qw} = U_{dc}$ and $\Delta E_c = E_{bc}$ parameters presented in Table 1 can serve as a criterion for the value of the internal electric field in a quantum well. Nonrectangular potential form provides in one's turn an additional shift of a low size quantization level in a range of the higher energy corresponding to the higher barrier tunneling transparency. Potential well in a Si layer is practically triangular at $\epsilon = 0$. If barrier width W_b is less than 2 nm, then electrons from quantum well can transport almost without difficulty with the lowest 2D states of the Si quantum well on the 3D states of the top $\text{Si}_{0.75}\text{Ge}_{0.25}$ barrier layer, thus providing relatively low electron mobility in the system and non-trivial behavior pattern of the temperature and magnetic-field dependencies in the samples.

Electron transport along a layer plane of the structure

The corresponding distribution of the electrons in the structure layers for the given sample is shown in Fig. 3. It is seen that electrons are localized only near the upper border of the well and their concentration can substantially exceed the average level of doping of the top barrier layer. The increase of size quantization levels in the narrow well to energies, where the barrier at the heterojunction is transparent for tunneling, can provide a variation of the measured transport properties of samples even for samples prepared at the same conditions. The observed instability, manifested during the transport measurements in high magnetic fields can be explained by interlayer tunneling transitions of 2D carriers from the quantum well to a three-dimensional state.

The most prominent feature of the observed magnetic field dependences of the $\text{Si}/\text{Si}_{1-x}\text{Ge}_x$

$x\text{Ge}_x$ heterostructures with a two-dimensional electron transport Si channel studied is the negative magnetoresistance (NMR) arising at low temperatures in a classical weak magnetic field [7]. It was shown in this work that in magnetic fields up to 2T the negative magnetoresistance can be explained by weak localization effect in 2D electron transport in the Si layer.

The typical form of the magnetic-field dependence of correction to conductivity $\Delta\sigma = \sigma(B) - \sigma_0$, where $\sigma_0 = \sigma(B = 0)$, observed in a weak magnetic field at low temperature about 5K for Sample 414 exhibiting highest conductivity is shown in Fig. 4.a. A part of the results represented by symbols - stars were obtained on samples being cut in the form of a square probe with alloyed contacts in low-temperature experiment with the use of inserts, placed in a dewar with liquid helium. Experimental data represented by symbols - points were obtained in a specialized liquid dilution cryostat (Oxford-instrument) on the bridge structures carved in the shape of a Greek cross. At zero magnetic field at liquid helium temperature conductivity of the Sample 414 was $\sigma_0 = 0.0056 \Omega^{-1}$. The line in Fig. 4.a approximating the experimental points is a polynomial curve, which shows a quadratic dependence of the observed correction to conductivity $\Delta\sigma = \sigma(B) - \sigma_0$ on the magnetic field:

$$\Delta\sigma/\sigma_0 \approx 0,00726 B^2. \quad (3)$$

The observed form of the dependence of correction to conductivity from the magnetic field points to the fact that in these heterostructures with high ($> 10^{12} \text{ cm}^{-2}$) surface electron density the magnetoresistance in weak magnetic field may be associated with the presence of a variety of mechanisms, including the existence of few groups of charge carriers in a system. These groups can be electrons distributed among different energy valleys of the conduction band of silicon layers as well as charge carriers in the top barrier layer of the structure.

It must be noted that NMR effect in a weak magnetic field is observed in the majority of the studied by us conductive SiGe/Si/SiGe heterostructures. The magnetic field dependence for different samples had often absolutely unexpected form. The most typical quadratic dependence (3) of the correction to the sample conductivity from magnetic field associated with existence of several carrier groups were observed in the samples with lowest resistance. The dependence $\Delta\sigma(B)$ for sample 413 have more complicated view as compared with sample 414 and can be approximated by formula:

$$\Delta\sigma/\sigma_0 \approx 0,5 B + 3,0 B^2 - 8,0 B^3 + 4,57 B^4. \quad (4)$$

Two-dimensional transport channel even doesn't arise in the structures with the insufficient elastic relaxation of the $\text{Si}_{1-y}\text{Ge}_y$ buffer layer. The resistance of these structures at temperatures below 20K reach megohms values. One could suppose that observing polysemantic character of the magnetic field dependence of the conductivity corrections in different samples is associated

with the different layer system deformation and reflects different contribution of some group of charge carriers, participating in the system conductivity.

The most reliable proof of the manifestation of two-dimensional properties of carriers in the system is the shape of the magnetic field dependences observed in the samples in strong quantizing magnetic fields. Low temperature measurements of the Hall effect and magnetoresistance in the magnetic fields up to 10T have been carried out on the samples having different scale of the elastic stress of Si channel and different level of plastic relaxation. Experimental data shown on the Fig. 4 have been obtained in a liquid dilution cryostat on the bridge 5x2 mm structures. The technology of this bridge preparation was described in [7].

The characteristic shape of the curves for one of the samples in magnetic fields up to 10T at liquid helium temperature is shown in Figs. 4.c and 4.d. The measurements were carried out in automatic regime at liquid helium temperature for positive and negative values of magnetic field and gating electric current about 3.7 μA . These measurements are characterized by the sizeable dispersion of the experimental points. The formation of the narrow potential barrier in the vicinity of the upper heterojunction enhances the probability of interlayer transitions of charge carriers in structures with a high doping level of the upper layer. In some cases, it has a noticeable effect on the transport characteristics of the system [7]. It can be assumed that the quite considerable scatter of points on the measured magnetotransport characteristics observed in our experiments is associated with the specifics of potential distribution in the layers of the investigated heterostructures, which makes possible an effective transfer of electrons between the possible parallel transport channels of the system. ***The increase of size quantization levels in the narrow well to energies, where the barrier at the heterojunction is transparent for tunneling, can provide a variation of the measured transport properties of samples even for samples prepared at the same conditions. The observed instability, manifested during the transport measurements in high magnetic fields can be explained by interlayer tunneling transitions of 2D carriers from the quantum well to a three-dimensional state.

Magnitudes of the measured resistances averaged on 10 adjacent points are presented on Figs. 4.c and 4.d. The lines in the figures have been obtained by fast Fourier-transformation procedure (FFT). Dependences of the resistance $R_{xx}(B)$ on magnetic field have good pronounced oscillating structure of the Schubnikov oscillation (Fig. 4.c), that allows to estimate the concentration of two-dimensional electrons in a Si channel. Calculations of the concentration density of the transport electrons in sample 414 using oscillating Schubnikov dependence let to estimate the value $n_{es} = (e/\pi\hbar)(\Delta N/\Delta B^{-1}) \approx (1-2)*10^{12} \text{ cm}^{-2}$, that corresponds to the surface electron concentration in this sample, found from Hall measurements in a weak magnetic field. For this structure Hall resistivity shows a series of weakly pronounced Hall steps in strong

magnetic fields, resulting from two-dimensional nature of some transport electrons participating in the system conductivity.

Diode characteristics of the structures for electron transport across the layers

The distribution of the potential as well as the distribution of charge carriers, along the direction perpendicular to the structure layers is traditionally studied using mesa diodes. If the external contact is ohmic, then the current-voltage (I-V) characteristics of the structure (Figs. 5.a and 5.b) is determined by the properties of the n-p junction on the boundary between the top n-Si_{1-x}Ge_x layer containing the Si transport channel and p-Si_{1-y}Ge_y variable buffer layer separating the active part of the structure from the substrate. The level of reverse currents through n-p junction characterizing its insulating properties is determined by the number of penetrating 60° dislocations on a contact area [12]. The properties of the n-p junction in the Si_{1-x}Ge_x layers, which doesn't contain intermediate Si layer, have been discussed in details in [13,14].

The thinness of the barrier formed at the heterojunction leads to the possibility of interlayer tunneling, even in non-resonant conditions. Interlayer tunneling can occur even, if there are local states, which may additionally lead to a resonant tunneling via the layers at lower electric fields in the vicinity of the heterojunction. Such a possibility, as an example of the output characteristics of the observed patterns of InGaAs/InAlAs transistor structure was first discussed in [10,11]. This mechanism may occur in the structures of silicon transistor type, especially when studying the features of the current flow across the plane of the structure [7]. The possibility of observation the falling section on the current-voltage characteristic of diode n⁺-SiGe/n-Si/p-SiGe heterostructure with Al ohmic contacts is shown in Figs. 5.c-5.f. The effect was observed only at temperatures below 120K at relatively low currents, corresponding mostly to the reverse branch of current-voltage characteristics.

Conclusions

The results of magnetoresistance and Hall measurements indicated the presence of a two dimensional electron gas in the studied n⁺-SiGe/n-Si/p-SiGe heterostructures. However, it has been concluded that the features of the magnetic field dependence and of the current-voltage characteristics can be explained by a variety of mechanisms, including the existence of few groups of charge carriers in a system and interlayer tunneling transitions of two-dimensional carriers from the quantum well to a three-dimensional state.

Acknowledgements

The work was carried out in cooperation between the Russian and Hungarian Academies of Sciences (project number 18) and with financial support from both the federal target program "Scientific and scientific-pedagogical personnel of innovative Russia" in 2009 -2013 years grant numbers 2012-1.2.1-12-000-2013-095 and 2012-1.3.1-12-000-2003-031; and the Russian Foundation for Basic Research project № 12-02-31567.

References

1. K. Ikeda, Y. Yamashita, A. Endoh, T. Fukano, K. Hikosaka, T. Mimura. *50-nm gate schottky source/drain p-MOSFETs with a SiGe channel*. // IEEE EDL, **23**, 670 (2002).
2. S.H. Olsen, K.S.K. Kwa, L.S. Driscoll, S. Chattopadhyay, A.G. O'Neill. *Design, fabrication and characterisation of strained Si/SiGe MOS transistors*. // IEE Proc. Circuits, Devices & Syst., **151**, 431 (2004).
3. J. Halstedt, M. von Haartman, P.E. Hellstrom, M. Ostling, H.H. Radamsson. *Hole mobility in ultrathin body SOI pMOSFETs with SiGe or SiGeC channel*. // IEEE EDL, **27**, 466 (2006).
4. R. Hull, J.C. Bean, D.J. Werder, R.E. Leibenguth. *In situ observations of misfit dislocation propagation in GeSi/Si(100) heterostructures*. // Appl. Phys. Lett., **52**, 1605 (1988).
5. K.W. Ang, K.J. Chui, V. Bliznetsov, C.H. Tung, A. Du, N. Balasubramanian, G. Samudra, M.F. Li, Y.C. Yeo. *Lattice strain analysis of transistor structures with silicon-germanium and silicon-carbon source/drain stressors*. // Appl. Phys. Lett., **86**, 093102 (2005).
6. E.B. Olshanetsky, V. Renard, Z.D. Kvon, J.C. Portal, N.J. Woods, J. Zhang, J.J. Harris. *Conductivity of a two-dimensional electron gas in a Si/SiGe heterostructure near the metal-insulator transition: Role of the short- and long-range scattering potential*. // Phys. Rev. B. **68**, 085304 (2003).
7. L.K. Orlov, Z.J. Horvath, M.L. Orlov, A.T. Lonchakov, N.L. Ivina, L. Dobos. *Anomalous electrical properties of Si/Si_{1-x}Ge_x heterostructures with an electron transport channel in Si layers*. // Physics of Solid State, **50**, N.2, 330 (2008).
8. T.G. Yugova, V.I. Vdovin, M.G. Milvidskii, L.K. Orlov, V.A. Tolomasov, A.V. Potapov, N.V. Abrosimov. *Dislocation pattern formation in epitaxial structures based on SiGe alloys*. // Thin Solid Films, **336**, 112 (1998).
9. M.M. Rieger, P. Vogl. *Electronic-band parameters in strained Si_{1-x}Ge_x alloys on Si_{1-y}Ge_y substrates*. // Phys. Rev. B. **48**, 14276 (1993).
10. M.L. Orlov, L.K. Orlov. *Mechanisms of negative resistivity and generation of terahertz radiation in a short-channel InGaAs/InAlAs transistor*. // Semiconductors, **43**, 652 (2009).
11. M.L. Orlov. *Mechanisms of a negative differential conductivity in a short – channel InGaAs/InAlAs HEMT*. // J. Phys: Conf. Ser., **193**, 012020 (2009).

12. Horváth Zs.J., Ádám M., Szabó I., Orlov L.K., Potapov A.V., Tolomasov V.A. Electrical behaviour of Al/SiGe/Si heterostructures: effect of surface treatment and dislocations.// Appl. Surf. Science, **234**, № 1-4, 54 (2004).
13. L.K. Orlov, Zs.J. Horvath, N.L. Ivina, V.I. Vdovin, E.A. Steinman, M.L. Orlov, Yu.A. Romanov. *Multilayer strained Si-SiGe structures: fabrication problems, interface characteristics and physical properties.* // Opto-Electronics Review, **11**, No.2, 169 (2003).
14. L.K. Orlov, Zs.J. Horvath, A.V. Potapov, M.L. Orlov, S.V. Ivin, V.I. Vdovin, E.A. Steinman, V.M. Phomin. *Electrical characteristics and the energy band diagram of the isotype n-SiGe/n-Si heterojunction in relaxed structures.* // Physics of Solid State, **46**, 2069 (2004).

Table 1. Characteristics of the potential barrier and quantum well formed in the conduction band for doping concentration $N_D = 2 \cdot 10^{18} \text{ cm}^{-3}$ (1,2) and $N_D = 1 \cdot 10^{18} \text{ cm}^{-3}$ (3-5) in the top $\text{Si}_{1-x}\text{Ge}_x$ layer and for the Si layer thickness $d_{\text{Si}} = 10 \text{ nm}$ (1-4) and 20 nm (5), as a function of relaxation level of elastic stress in the layers, determining band offsets ΔE_v and ΔE_c at the interfaces.

№	ε (%)	d_{Si} nm	ΔE_v meV	$\Delta E_c = E_{bc}$ meV	$h_b = E_{ba}$ meV	$dE_{\text{qw}} = U_{\text{dc}}$ meV	$W_b = X_{\text{fe}}$ nm	$W_{\text{qw}} = X_{\text{ee}'}$ nm	$W_{\text{qw}} = X_{\text{bb}'}$ nm
1	100	10	56	190	146	82	1.9	10	10
2	0	10	178	62	55	65	1,3	3.8	9.4
3	100	10	56	190	146	68	5.0	10	10
4	0	10	178	62	49	54	3,2	5.9	10
5	100	20	56	190	148	100	5.2	20	20

Figure captions

Fig. 1. The distribution of Si and Ge alloy components across the SiGe/Si/SiGe structure with the Si transport channel $d_{Si} \approx 8$ nm (left) and the electron microscopic image of the structure 412 (right).

Fig. 2. The structure of the energy bands (valence band (v) and conduction band (c)) (a,b) and the distribution of electron density n_e in the structure layers (c,d) across the relaxed (a,c) and no relaxed (b,d) $Si_{0.75}Ge_{0.25}/Si/Si_{0.75}Ge_{0.25}$ heterostructures. The calculations have been carried out for the donor concentration $N_D = 2 \cdot 10^{18} \text{ cm}^{-3}$ in the $Si_{0.75}Ge_{0.25}$ top barrier layer and for the elastic strain of Si layer ($d_{Si} = 10$ nm) $\epsilon = 100\%$ (a,c) and $\epsilon = 0\%$ (b,d), that correspond to the option at $T=300^\circ\text{C}$ of the next parameters of the contacting materials [11]: $E_g(\text{Si}) = 0.93$ eV (a,c), 1.1 eV (b,d), $E_g(\text{Si}_{0.75}\text{Ge}_{0.25}) = 1.07$ eV (a,c), 0.986 eV (b,d), $\Delta E_v = 0.056$ eV (a,c), 0.178 eV (b,d).

Fig. 3. Potential of quantum well in Si layer (a), distribution of the electron density n_e/N_D (b,c,d)), in the structure, referred to the donor concentration N_D in the top barrier layer for $Si_{0.75}Ge_{0.25}/Si/Si_{0.75}Ge_{0.25}$ heterostructures with a maximum stress ($\epsilon = 100\%$: a,b,(c-f) – symbol star) and no stress ($\epsilon = 0\%$: (c-e) – symbol circle) with Si layer with thickness 10 nm and N_D ($I = 10^{18} \text{ cm}^{-3}$; c) the width of the barrier at the interface of layers, d) maximum electron concentration in a quantum well, and e,f) the value of the quantum well parameters for different energy depends from depending of a top barrier layer.

Fig.4. The magnetic-field dependence of correction to conductivity $\Delta\sigma$ for the two samples at $T = 4.2\text{K}$ in a weak magnetic field (a,b). Symbols - experimental data, line - approximating parabola. Magnetoresistance (c) and Hall (d) characteristics of the structure 414 in a magnetic strong field. Open symbols represents the averaged experimental data. The lines in the figures obtained by smoothing the experimental data .

Fig.5. Transverse current-voltage characteristics of the diode n-SiGe/p-Si (a) structure and modulation - doped n^+ -SiGe/n-Si/p-SiGe transistor structures measured on several mesa diodes with *** contacts at temperatures 100 K (solid symbols) and 300 K (open symbols) and with Al ohmic contacts at 80K (b-curve 1, d), 100K (c,e), 120K (b-curve 2),(f), and 200K (b-curve 3).

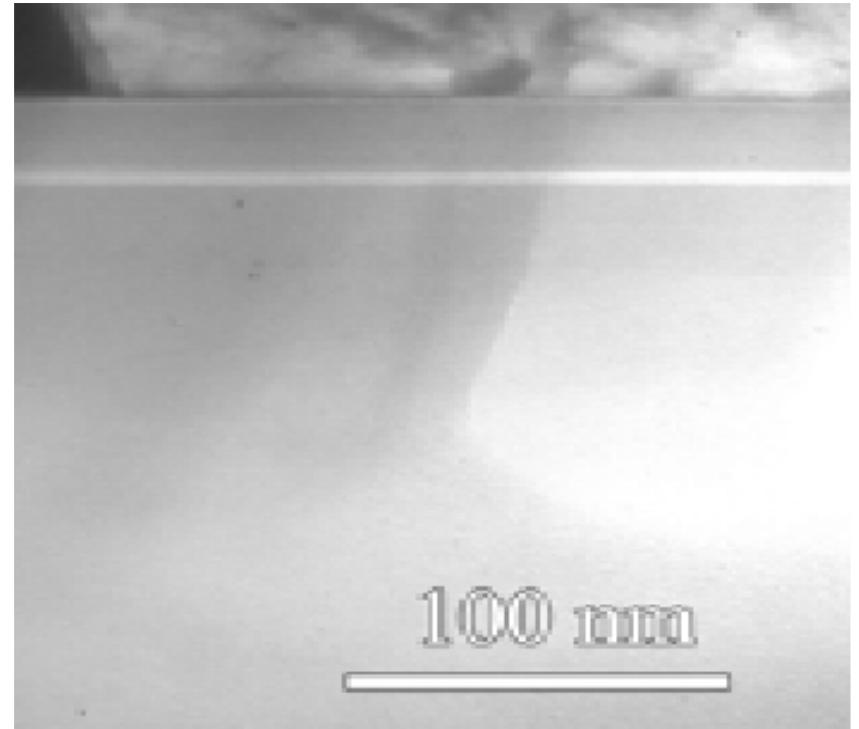
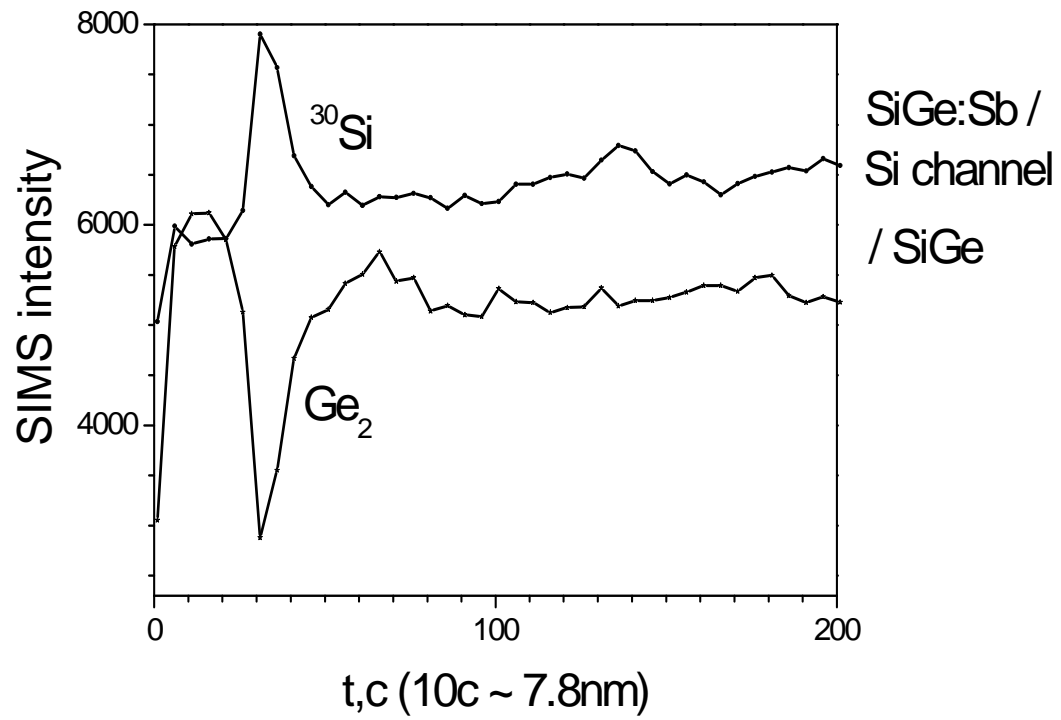


Fig. 1

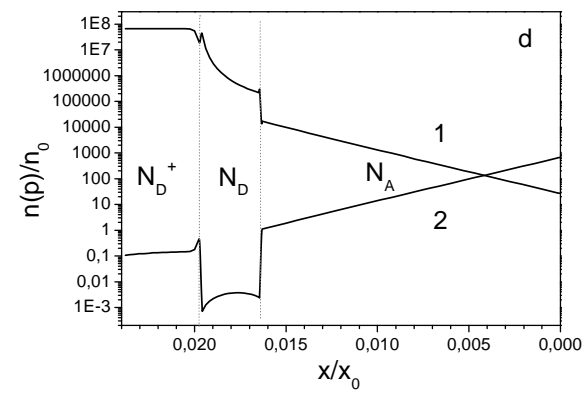
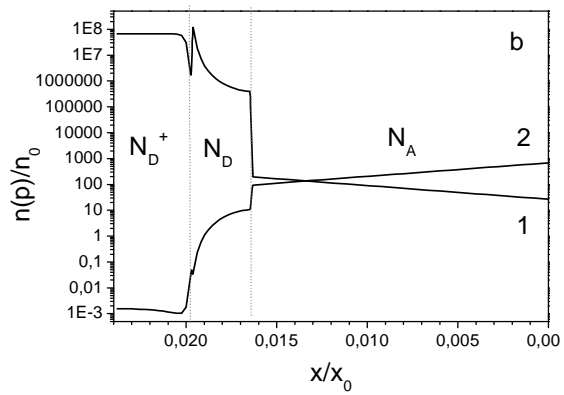
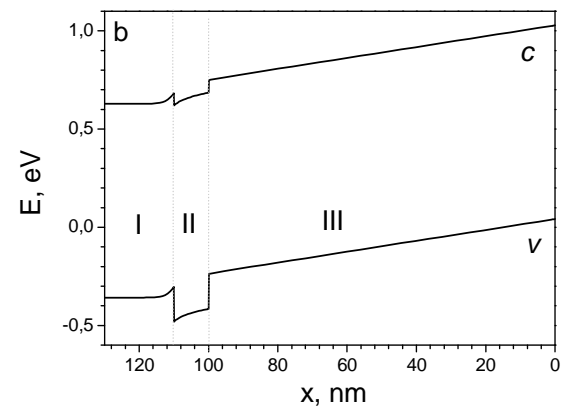
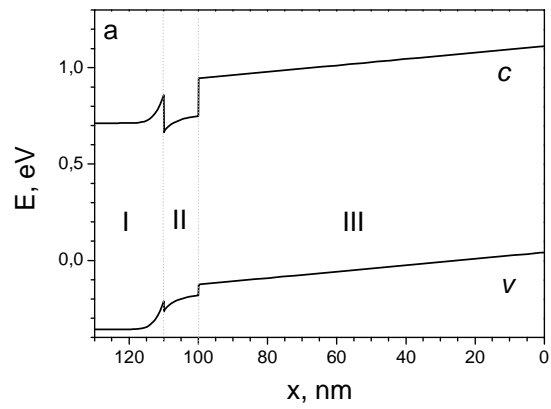


Fig. 2

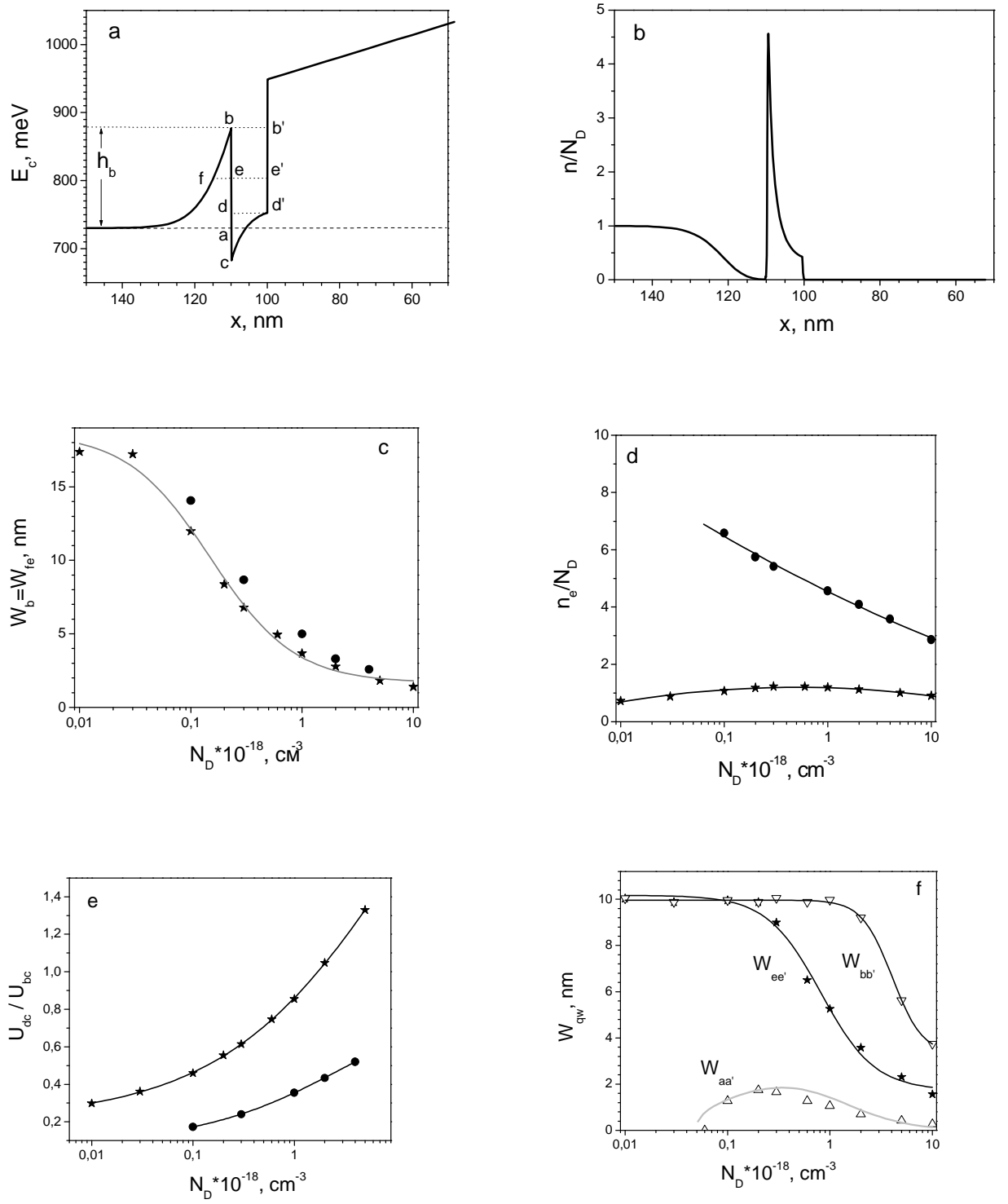


Fig. 3

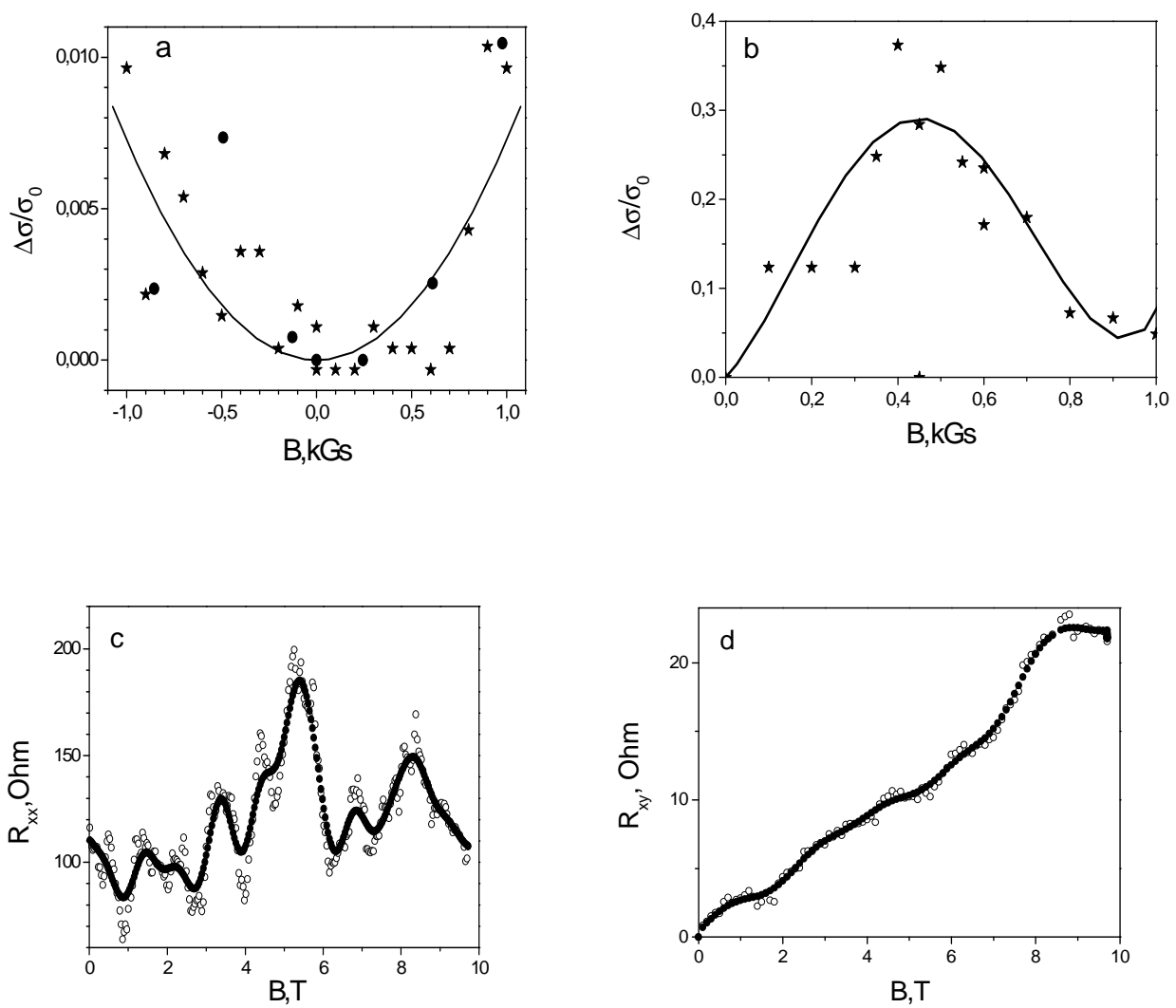


Fig. 4

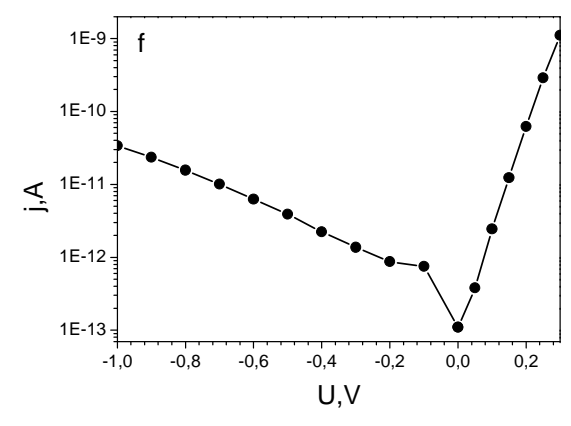
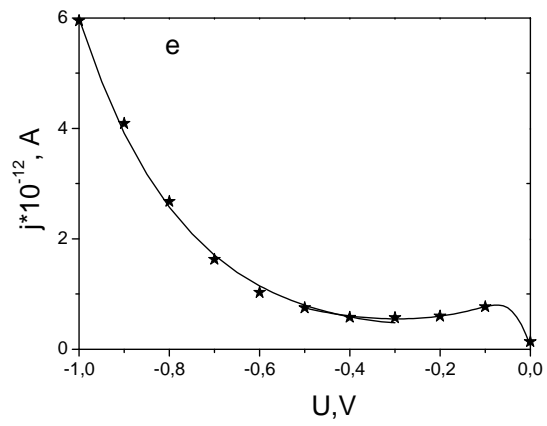
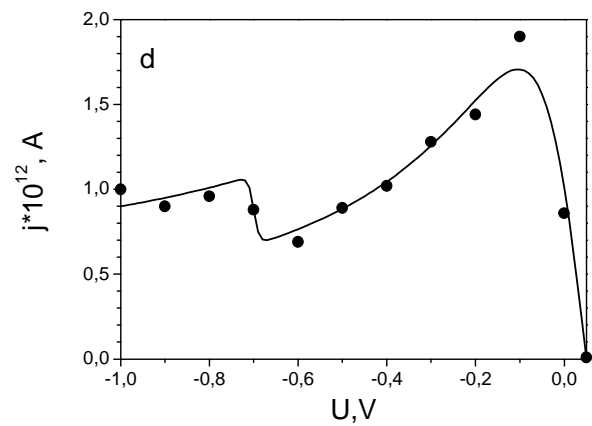
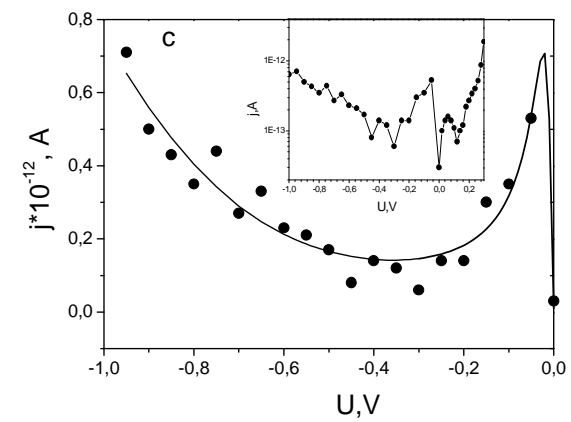
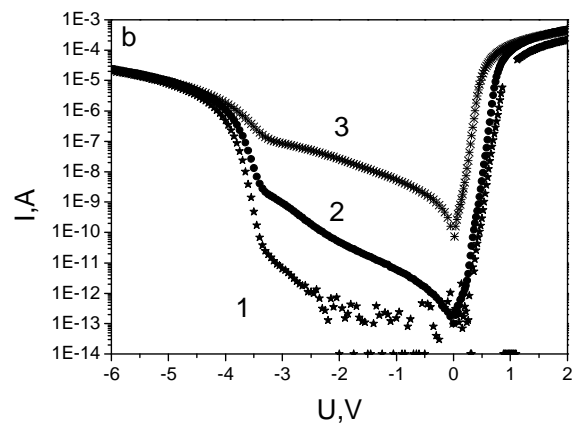
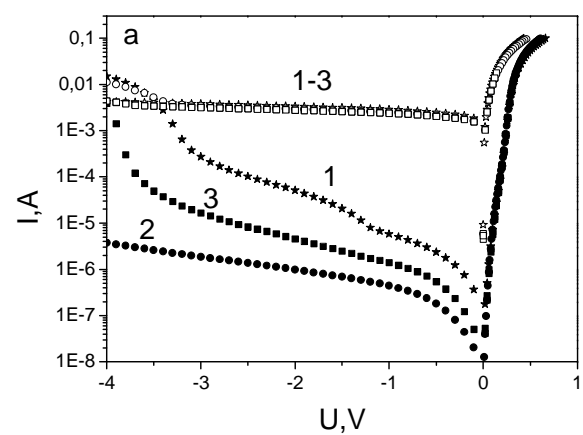


Fig. 5